Proceeding of the IEEE
International Conference on Robotics and Biomimetics (ROBIO)
Shenzhen, China, December 2013

Performance Evaluation of the Wireless Microrobot in pipe with Symmetrical Spiral Structure

Jian Guo, Xiang Wei, Shuxiang Guo, Wei Wei, Yuehui Ji and Yunliang Wang

Abstract—**A wireless microrobot may be used in the small space and biomedical practice, especially in the industrial field and biomedical application. In this paper, we designed a new kind of wireless microrobot with symmetrical spiral structure, which have more compact volume, completely symmetrical mechanical structure, quick response, forward-backward motions and can clean the dirt adhering to the inner wall. According to the hydromechanical lubrication theory and Newton viscous law, we build the motion model of the microrobot. Through analysis, simulations and experiments, this paper had evaluated the effect of spiral depth and thread unit number. In addition, we verified the feasibility of this new kind of microrobots, and obtained the moving speeds of forward-backward and upward-downward motion in the pipe. The experimental results indicated that the maximum moving speed is 22.68 mm/s at 12 Hz in the horizontal direction and 6.29 mm/s at 13Hz in the vertical direction with input currents of 0.7A. Finally, we designed a control panel for this system, which can control the microrobot current motion states easily, and make our system more portable and compact. The designed wireless microrobot can move smoothly in water and other liquid medium and is very useful in the industrial application and microsurgery application.**

I. Introduction

ENDOVASCULAR intervention has become more and more popular in recently. It is widely used in biomedical practice, diagnosis and surgery. Pipeline micro-robot is an important research branch of MEMS (Micro-Electro-Mechanical System). Gastrointestinal (GI) endoscopy is widely carried out in order to find diseases at their early stages such as stomach and colon cancer, ulcerative colitis, etc. To minimize the suffering of a patient, a capsule endoscope has been developed [1]. The capsule swallowed by the patient can transmit pictures of an internal GI tract wirelessly. With the aid of peristalsis, it moves passively through GI tract. However, the capsule cannot control its moving direction and moving speed itself, due to the waste of large quantities of data. So the capsule endoscope needs an autonomous moving function.

In order to safely and reliably complete the intestinal examination and surgical operations, and to reduce the suffering of the patients, several kinds of microrobots have been developed for various purposes owing to advances in precise process technology, and further progress in this field is expected [2]-[4]. However, because they cannot be driven wirelessly, they are difficult to use for a moving device such as the capsule endoscope.

In our previous study, as wireless microrobots controlled by a external magnetic field are both safe and reliable, and can be carried deep within the tissues of living organisms in the body fluids, it is need to propose a new kind of magnetic field model to drive the microrobot easily [5]-[7]. With the different kinds of external magnetic field driven, there are many locomotion forms are proposed. For example the fish-like motion, paddle motion, propeller-driven motion and spiral motion [8]-[14]. In so many kinds of motions, we can find that the kind of spiral motion, which not only can obtain the maximum driving force, but also is the highest efficiency in a very small space.

So in this paper, we designed a rotation magnetic field model to establish external magnetic field, and design a kind of microrobot with a symmetrical spiral structure. The organization of this paper is as follow. In section 2, presented the design, modeling and analysis of the microrobot with a symmetrical spiral structure we proposed before. Section 3, showed the simulation and experimental results of our designed microrobots. And finally, we made a conclusion and talked about future work.

II. The Proposed Wireless Microrobot

A. The structure of the wireless microrobot

The spiral type of microrobot has been designed in the previous study, but it contains four pieces of permanent magnets, and the rotation mechanism is separate with the main body of microrobot. In this paper, we proposed a new kind of spiral type of microrobots, which only contain one piece of permanent magnets, and had a more compact structure [14].

Fig. 1 has shown the structure of the prototype of wireless microrobot which consists of two main parts. In order to ensure the balance of the microrobot, we developed a completely symmetrical structure, which can also achieve the

Manuscript received August 31, 2013.

Jian Guo and Xiang Wei is with Tianjin Key Laboratory for Control Theory & Application in Complicated Systems and Biomedical Robot Laboratory, the School of Electrical Engineering, TianJin University of Technology, TianJin, China (e-mail: gj15102231710@163.com; weixiang_tjut@163.com).

Shuxiang Guo is with the Intelligent Mechanical Systems Engineering Department, Kagawa University, Takamatsu, Kagawa, Japan. He is also with Tianjin Key Laboratory for Control Theory & Application in Complicated Systems and Biomedical Robot Laboratory, the School of Electrical Engineering, TianJin University of Technology, TianJin, China (e-mail: guo@eng.kagawa-u.ac.jp).

Wei Wei, Yuehui Ji and Yunliang Wang is with Tianjin Key Laboratory for Control Theory & Application in Complicated Systems and Biomedical Robot Laboratory, the School of Electrical Engineering, TianJin University of Technology, TianJin, China (e-mail: weiweilove20000@163.com; wangyl@tjut.edu.cn).

978-1-4799-2744-9/13/$31.00 ©2013 IEEE

same kinematic characteristics.

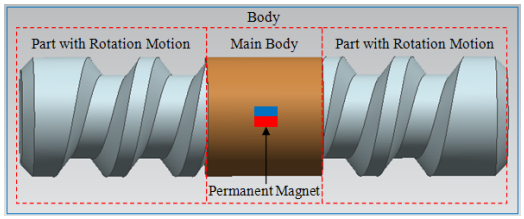

Fig. 1. The structure of the proposed microrobot

B. The modeling of the microrobot

According to the right-hand rule, we established the coordinate system for the microrobot movement as shown in Fig. 2. In the right-hand coordinate system, V is the axial velocity, U is the circumferential velocity. For the sake of analysis the force effect of the microrobot, we assumed the direction of the screw thread is x-axis, the thickness direction of the screw thread is y-axis, the direction which is vertical to the microrobot body is z-axis, and θ is the spiral angle. U and V can be composed of u_x (x-component) and w_z (z-component).

$$u_x = U\sin\theta + V\cos\theta \tag{1}$$

$$w_z = V\sin\theta - U\cos\theta \tag{2}$$

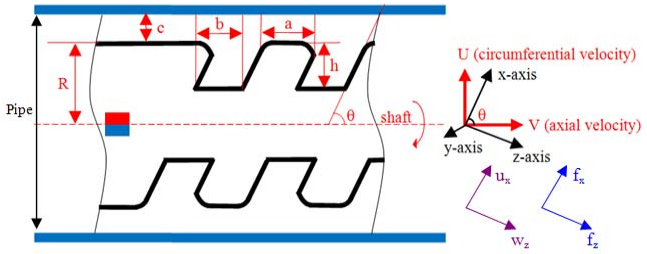

Fig. 2. Conceptual structure of the screw thread

In the previous study, based on hydromechanical lubrication theory and Newton viscous law, the similar force analysis had been discussed [13]. According to our designed microrobot in the pipe, the main force will be evaluated as shown in the Table Ⅰ in the horizontal direction, which consists of f_x ,f_z, F_{axial}, F_{circum}, $f_{l\text{-}resist}$ and $f_{r\text{-}friction}$. And in the vertical direction, the G and F_u should be considered separately.

TABLE I
EXPLANATION OF THE MAIN FORCE

Main force	Explanation
f_x	The total shear stress of the screw thread gap region and the thread region in x-axis.
f_z	The total shear stress of the screw thread gap region and the thread region in z-axis.
F_{axial}	The axial traction force.
F_{circum}	The circumferential friction force.
$f_{l\text{-}resist}$	The resistance from the liquid.
$f_{r\text{-}friction}$	The rolling friction between the mircrobot and pipe
G	The weight of the microrobot
F_u	The buoyancy of the microrobot in the liquid

According to Newton viscous law, we can obtain the f_x and f_z as following:

$$f_x = \mu A\frac{du}{dy} = -n\mu(U\sin\theta + V\cos\theta)\left(\frac{a}{c}+\frac{b}{c+h}\right) \tag{3}$$

where n is the number of thread unit, μ is the viscosity coefficient of the liquid, A is the contact area, du/dy is the velocity gradient.

$$f_z = -n\mu w_z\left[\frac{3abh^2}{bc^3+a(c+h)^3}+\frac{a}{c}+\frac{b}{c+h}\right] \tag{4}$$

Then we can compute the axial traction force, circumferential friction force, resistance from liquid as following:

$$F_{axial} = f_x\cos\theta + f_z\sin\theta = \frac{3n\mu abh^2(U\sin\theta\cos\theta - V\cos^2\theta)}{bc^3+a(c+h)^3} - n\mu V\left(\frac{a}{c}+\frac{b}{c+h}\right) \tag{5}$$

$$F_{circum} = f_z\cos\theta - f_x\sin\theta = \frac{3n\mu abh^2(U\cos^2\theta - V\sin\theta\cos\theta)}{bc^3+a(c+h)^3} + n\mu U\left(\frac{a}{c}+\frac{b}{c+h}\right) \tag{6}$$

$$F_{l\text{-resist}} = 0.5k\rho V^2 S = 0.5k\rho V^2\pi R^2 \tag{7}$$

$$F_{r-fricition} = \eta G \tag{8}$$

$$G = m_g g \tag{9}$$

$$F_u = \rho g V_g = \frac{\rho}{\rho_g}G \tag{10}$$

where k is the damping coefficient of the liquid, ρ is the density of the liquid, S is the front of contact area of the microrobot, η is the coefficient of rolling friction, G is the weight of the microrobot, V_g is the volume of the microrobot, ρ_g is the density of material used to design the microrobot.

We can obtain mg from an electronic balance, and calculate G and F_u easily. In order to simplify the equations, we assumed β=a /a+b, γ=h/c, so we can obtain:

$$\overline{F}_{axial} = F_{axial}\cdot\frac{c}{a+b} = \frac{3n\mu\beta(1-\beta)\gamma^3(U\sin\theta\cos\theta - V\sin^2\theta)}{(1-\beta)+\beta(1+\gamma)^3} - nV\mu\left(\beta+\frac{1-\beta}{1+\gamma}\right) \tag{11}$$

$$\overline{F}_{circum} = F_{circum}\cdot\frac{c}{a+b} = \frac{3n\mu\beta(1-\beta)\gamma^3(U\cos^2\theta - V\sin\theta\cos\theta)}{(1-\beta)+\beta(1+\gamma)^3} + nU\mu\left(\beta+\frac{1-\beta}{1+\gamma}\right) \tag{12}$$

Therefore, the total force of the microrobot in the horizontal direction in-pipe is:

$$F_{horizontal} = \overline{F}_{axial} + \overline{F}_{circum} - F_{l-resist} - F_{r-friction} \tag{13}$$

In the vertical motion, the microrobot is also influenced by its gravity and the buoyancy from the liquid, we assumed ΔF=F_u-G, so the total force of the microrobot in the vertical direction in-pipe is:

$$F_{vertical} = \overline{F}_{axial} + \overline{F}_{circum} + \Delta F - F_{l-resist} - F_{r-friction} = F_{horizontal} + \Delta F \tag{14}$$

When the traction force is zero, the axial speed is maximal,

the expression of maximum speed as following [16]:

$$V_{\max} = \frac{3n\beta(1-\beta)\gamma^3 \sin\theta\cos\theta}{\left(\beta+\frac{1-\beta}{1+\gamma}\right)\left[(1-\beta)+\beta(1+\gamma)^3\right]+3\beta(1-\beta)\gamma^3\sin^2\theta}\cdot U = f(\beta,\gamma,\theta) \quad (15)$$

C. The motion analysis of the microrobot in the horizontal direction

We had simulated the performance effect of the spiral depth h to F_{axial}, F_{circum}, $f_{l\text{-}resist}$, $f_{r\text{-}friction}$, $F_{horizontal}$ and V_{max}. By refer to the structure of microrobot we designed, we assumed β=0.5, μ=0.001, U=0.05, V=0.5, n=2, k=1, ρ=1, R=0.006, θ=π/4. Considered of the size of the microrobot, we fixed the range of γ is 0 to 10. The simulation results in the horizontal direction as shown in Fig. 3 and Fig. 4.

From the results, we conclude that when h/c>=1 and f_{axial}>0, the traction force of capsule is positive. When h/c=1, f_{circum} has the minimum value. The V_{max} will increase as γ increases. When γ is equal to 8, the V_{max} will increase slowly and reach a fixed maximum value finally.

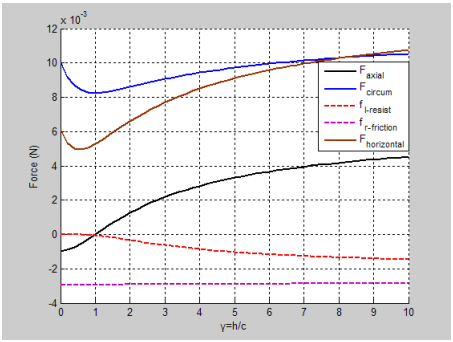

Fig. 3. The curves of F_{axial}, F_{circum}, $f_{l\text{-}resist}$, $f_{r\text{-}friction}$, $F_{horizontal}$ when γ changes

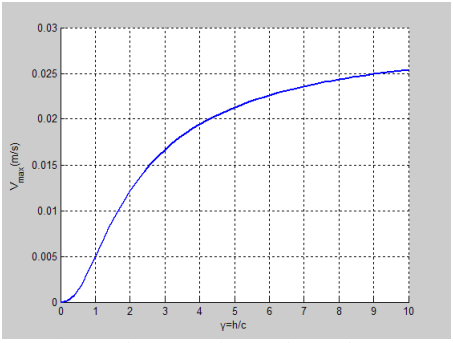

Fig. 4. The curve of V_{max} when γ changes

If we make the assumption that β=0.5, γ=3, μ=0.001, U=0.05, V=0.5, k=1, ρ=1, R=0.006, θ=π/4 and the simulation results are shown in Fig. 5.

From the results, we conclude that when number of thread unit is 5, $F_{horizontal}$ is the maximum value.

D. The motion analysis of the microrobot in the vertical direction

We had also simulated the performance effect of the spiral depth h in the vertical direction. We assumed β=0.5, μ=0.001, U=0.05, V=0.5, n=2, k=1, ρ=1, ρg=1.1, R=0.006, θ=π/4. Considered of the size of the microrobot, we fixed the range of n is 0 to 10. The simulation results as shown in Fig. 6.

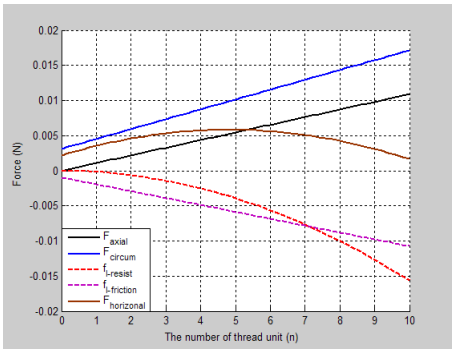

Fig. 5. The curves of F_{axial}, F_{circum}, $f_{l\text{-}resist}$, $f_{r\text{-}friction}$, $F_{horizontal}$ when n changes

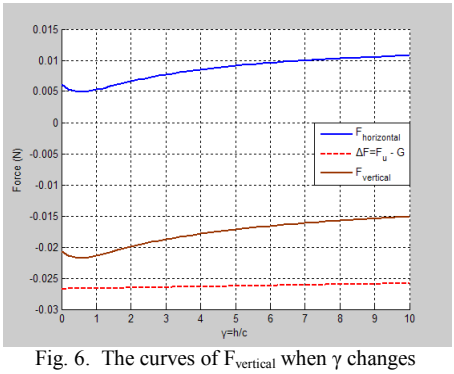

Fig. 6. The curves of $F_{vertical}$ when γ changes

If we make the assumption that β=0.5, γ=3, μ=0.001, U=0.05, V=0.5, k=1, ρ=1, ρ_g=1.1, R=0.006, θ=π/4 and the simulation results are shown in Fig. 7.

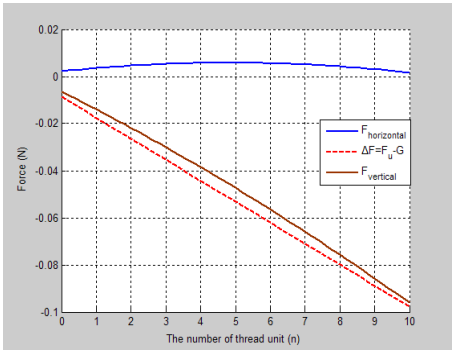

Fig. 7. The curves of $F_{vertical}$ when n changes

From (14) and result, we can find that $F_{vertical}$ is just related to $F_{horizontal}$ and ΔF, but the $F_{vertical}$ is a negative value. So the microrobot cannot achieve upward motion, and needs gravity compensation.

III. Experiments and Results

A. Experiment on the forward-backward motion

In the detection process, the microrobot should complete forward-backward motion in the pipe. Based on the theoretical analysis of the proposed microrobot in our previous study [15], we had proved it can move forward and backward in a pipe. So we developed the new kind of spiral type microrobot, it is shown in Fig. 8.

By using the measurement system as shown in Fig. 9, the following characteristics of the moving speed were measured. We carried out the experiments by changing the frequency of input currents from 0 Hz to 15 Hz, and the amplitude of input

currents were fixed at 0.7 A.

Fig. 8. Prototype of the microrobot

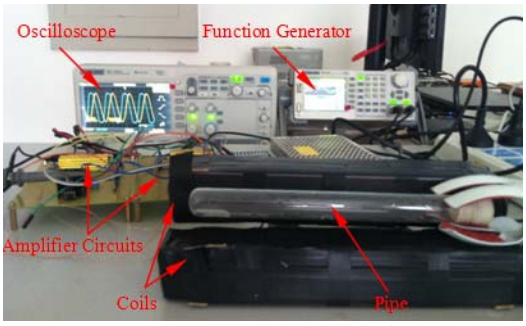

Fig. 9. Measurement system in horizontal experiment

Based on the measurement system, the microrobot can achieve rotation motion in the pipe forward-backward. Through changing the frequency and phase of input currents, the experimental results of average moving speed of the microrobot were obtained as shown in Fig. 10.

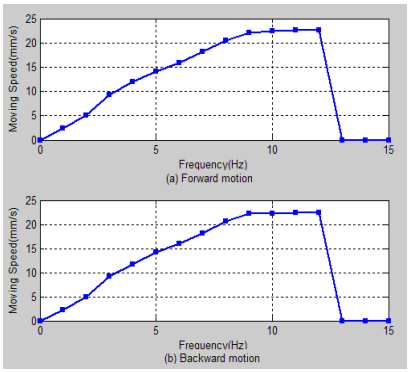

Fig. 10. Moving speed of forward-backward motion

B. *Experiment on the upward-downward motion*

According to our preceding analysis and the simulation results in Fig. 6 and Fig. 7, we can conclude that the $F_{vertical}$ is a negative value ,so the microrobot cannot realize upward motion in the pipe, and we should counterweight for the microrobot in order to make $\Delta F=0$, which is let the microrobot suspend in water.

Considered the material of the microrobot, we select another material that has a small density as gravity compensation. The specifications of materials are shown in Table Ⅱ and Fig. 11.

TABLE Ⅱ
SPECIFICATIONS OF MATERIALS

Part	Main material	Density (g/cm^3)
Body	EVA (Ethylene Vinyl Acetate)	1.1
Permanent magnet	NdFeB	6
Gravity compensation	EPE (Expandable Polyethylene)	0.003

In addition, the EPE is a kind of very soft material, which installs at the head and end of the microrobot will buff the microrobot impact the pipeline, so that will improve the safety of detection process. The prototype of the microrobot with gravity compensation is shown in Fig. 12.

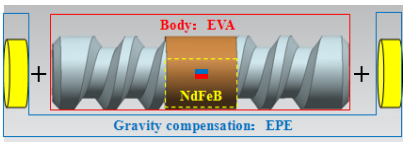

Fig. 11. The gravity compensation of the microrobot

Fig. 12. Prototype of the microrobot with gravity compensation

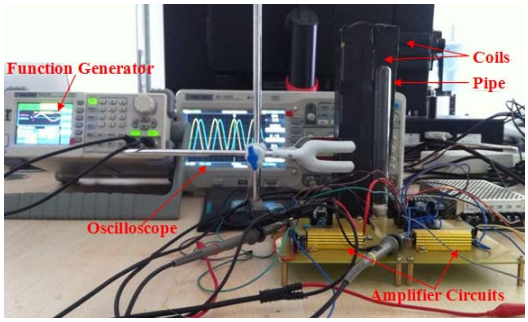

Fig. 13. Measurement system in vertical experiment

Based on the measurement system as shown in Fig. 13, the microrobot can achieve upward-downward motion in the pipe. Through changing the frequency and phase of input currents, the experimental results of average moving speed of the microrobot were obtained as shown in Fig. 14.

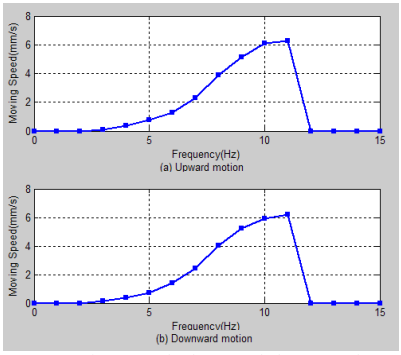

Fig. 14. Moving speed of upward-downward motion

Seen from Fig. 10 and Fig. 14, it is finding that this kind of microrobots with symmetrical structure has the similar kinematic characteristics on the forward-backward and upward-downward motion. These symmetrical characteristics will make the control strategy much easier.

C. *Experiment on the developed microrobots with different spiral depth h*

We had developed four types of microrobots with different spiral depth h that 3mm, 4mm, 5mm and 6mm, which had the same spiral unit number 5. The prototypes of the microrobot are shown in Fig. 15 and the specification of the spiral structures are shown in Table Ⅲ.

Based on the experimental measurement system, we

measured the moving speeds of different spiral depth of the microrobots in the horizontal direction. By changing the frequency of the input currents from 0 Hz to 15 Hz, and the amplitude of input currents were fixed at 0.7 A, the experimental results of average speeds were obtained as shown in Fig. 16.

Seen from Fig. 16, it is conclude that the moving speed of microrobot will increase as the frequency increases of input currents. And when the spiral depth is deepened, the maximum speed will be accelerated, but the frequency range will be decreased.

TABLE Ⅲ
SPECIFICATIONS OF PROTOTYPE MICROROBOTS

	Size	Spiral depth h
Microrobot 1	Φ12mm×60mm	3mm
Microrobot 2	Φ12mm×60mm	4mm
Microrobot 3	Φ12mm×60mm	5mm
Microrobot 4	Φ12mm×60mm	6mm

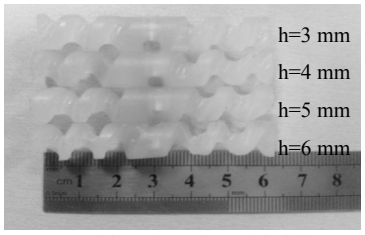

Fig. 15. Prototypes of the microrobot with different spiral depth

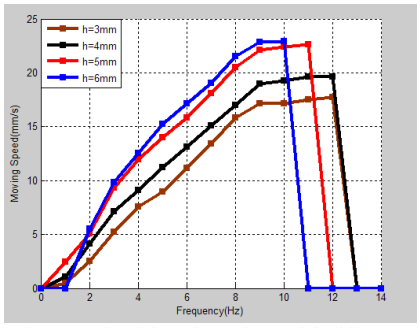

Fig. 16. Moving speeds of the microrobots with different spiral depth

Seen from Fig. 16, it is conclude that the moving speed of microrobot will increase as the frequency increases of input currents. And when the spiral depth is deepened, the maximum speed will be accelerated, but the frequency range will be decreased.

In addition, when the frequency of the input currents over 13 Hz, the moving speed of the microrobots in pipe is down to zero. This is because of the limitation of magnetic field intensity, and the wireless microrobots cannot rotate following the rotation magnetic field at a high level frequency any more, so the microrobots will out-of-step with the rotation magnetic field.

D. Experiment on the developed microrobots with different thread unit numbers n

We had developed five types of microrobots with different thread unit numbers n that 3, 4, 5, 6 and 7, which had the same spiral depth 5mm. The prototypes of the microrobot are shown in Fig. 17, and the specification of the spiral structures are shown in Table Ⅳ.

We also measured the moving speeds of different thread unit numbers of the microrobots in the horizontal direction. By changing the frequency of the input currents from 0 Hz to 15 Hz, and the amplitude of input currents were fixed at 0.7 A, the experimental results of average speeds were obtained as shown in Fig. 18.

TABLE Ⅳ
SPECIFICATIONS OF PROTOTYPE MICROROBOTS

	Size	Thread unit number n
Microrobot 5	Φ12mm×40mm	3
Microrobot 6	Φ12mm×50mm	4
Microrobot 7	Φ12mm×60mm	5
Microrobot 8	Φ12mm×70mm	6
Microrobot 9	Φ12mm×80mm	7

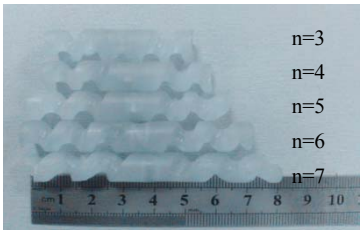

Fig. 17. Prototypes of the microrobot with different thread unit numbers

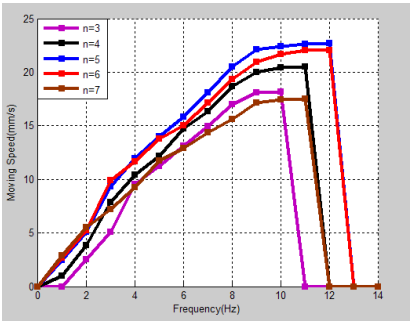

Fig. 18. Moving speeds of the microrobots with different thread unit numbers

Seen from Fig. 18, it is conclude that the moving speed of microrobot will increase as the frequency increases of input currents. And when the number of thread unit is 5, the microrobot can achieve the maximum moving speed and frequency range.

E. Design of control panel for the system

In the experimental stage, we use a function generator to generate sine wave signals, but not portable and compact. Based on the experimental results, we design a control panel for our system.

The control panel we designed is shown in Fig. 19. Through selection of the buttons, we input the status we needed, and then the MCU will output the corresponding signals to the amplifying unit and display the current status. The control panel can realize stopping, running and changing the direction of motion, which can be selected through the button control. In the running status, we can choose low-speed motion, mid-speed motion and high-speed motion.

With this control panel, we can control the microrobot

current motion states easily, and the moving speed can be selected by the experimental results.

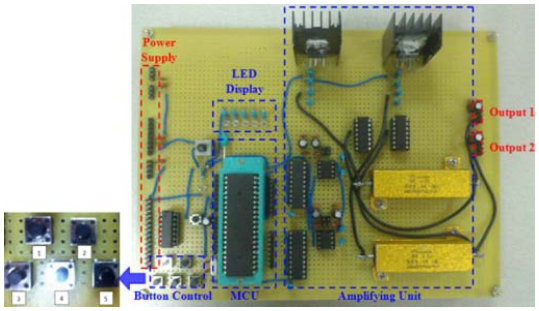

Fig. 19. Control panel (Button control: 1.Start/ Stop, 2.Motion direction control, 3.Low-speed motion, 4.Mid-speed motion, 5.High-speed motion)

IV. Conclusion and Future Work

In this paper, a new kind of wireless microrobots in pipe with symmetrical spiral structure has been designed. This paper has discussed the wireless microrobot structure, motion mechanism and kinematic characteristics evaluation of it. In order to evaluate the performance of the spiral structure, we also developed microrobots with different spiral depth and different thread unit numbers. The experimental results indicated a number of advantages of the developed wireless microrobot as:

[1] This kind of wireless microrobots with symmetrical spiral structure we designed had a more compact mechanical structure and symmetrical kinematic characteristics with a very simple and efficiency control strategy.

[2] Based on hydromechanical lubrication theory and Newton viscous law, we modeled and analyzed the performance effect of the spiral depth and thread unit number to the kinematic characteristics of the microrobot.

[3] Based on the theoretical analysis and experiments, we had verified that the wireless microrobot with gravity compensation can move forward-backward and upward-downward in the pipe, and could stop at any position we needed.

[4] The experimental results showed that the maximum moving speed is 22.68 mm/s at the frequency of 12 Hz in the horizontal direction and 6.29 mm/s at the frequency of 13Hz in the vertical direction with currents of 0.7A based on the type of Mircorobot 7, which is the optimal structure in this kind of wireless microrobot with symmetrical structure.

[5] In order to realize portable and compact control, we designed a control panel, which can achieve stopping, running and changing the direction of motion. And in the running status, we can choose low-speed motion, mid-speed motion and high-speed motion.

In the future, we will focus on reducing the volume of the microrobot, and make it suitable for a more small space to work. It is also need to establish a more DOFs experimental system to realize the microrobot more DOFs motion in the pipe.

This kind of microrobot will play an important role in industrial and biomedical applications, for example, to conduct in-pipe inspections. It also possesses a high potential for applying for the microsurgery of blood vessels and in minimally invasive biomedical procedures.

Acknowledgment

This research is supported by Key Research Program of the Natural Science Foundation of Tianjin （13JCZDJC26200）
.

References

[1] G. Iddan, G. Meron, A. Glukhovsky, and P. Swain, “Wireless capsule endoscopy,” International Journal of Nature, Vol.4, pp. 717-719, 2000.

[2] L. Phee, D. Accoto, A. Menciassi, C. Stefanini, M. C. Carrozza, and P. Dario, “Analysis and development of locomotion devices for the gastrointestinal tract,” Proceedings of the 2002 IEEE Transactions on Biomedical Engineeriong, Vol. 49, pp.613–616, 2002.

[3] H. D. Høeg, A. B. Slatkin, J.W. Burdick, and W. S. Grundfest, “Biomechanical modeling of the small intestine as required for the design and operation of a robotic endoscope,” Proceedings of the 2000 IEEE International Conference on Robotics & Automation, pp.1599–1606, 2000.

[4] K. Ikeuchi, K. Yoshinaka, and N. Tomita, “Low invasive propulsion of medical devices by traction using mucus,” International Journal of Wear, Vol. 209, pp.179–183, 1997.

[5] M. Sendoh, K. Ishiyama, and K. I. Arai, “Direction and individual control of magnetic micromachine,” Proceedings of the IEEE Transactions on Magnetics, vol. 38, pp.3356–3358, 2002.

[6] Y Zhang, H Xie, N Wang, “Design, analysis and experiments of a spatial universal rotating magnetic field system for capsule robot,” Proceedings of 2012 IEEE International Conference on Mechatronics and Automation, pp.998-1003, 2012.

[7] Tan R, Liu H, Su G, “Experimental investigation of the small intestine's viscoelasticity for the motion of capsule robot,” Proceedings of the 2011 IEEE International Conference on Mechatronics and Automation, pp.249-253, 2011

[8] S Guo, Y Sasaki, Fukuda T, “A New Kind of Microrobot in Pipe Using Driving Fin”, Proceedings of the 2003 IEEE/ASME International Conference on Advanced Intelligent Mechatronics, Vol. 2, pp.667-702, 2003.

[9] S Guo, Q Pan, “Mechanism and Control of a Novel Type Microrobot for Biobiomedical Application”, Proceedings of the 2007 IEEE International Conference on Robotics and Automation, pp.187-192, 2007.

[10] S Guo, Q Pan, Khamesee M B, “Development of a novel type of microrobot for biobiomedical application”, Journal of Microsystem Technologies, Vol.14, No.3, pp.307-314, 2008.

[11] Q Pan, S Guo, “A Paddling type of microrobot in pipe”, Proceedings of the 2009 IEEE International Conference on Robotics and Automation pp.2995-3000, 2009.

[12] Q Pan, S Guo, Okada T, “A Novel Hybrid Wireless Microrobot”, International Journal of Mechatronics and Automation, Vol.1, No.1, pp.60-69, 2011.

[13] T Okada, S Guo, N Xiao, “Control of the wireless microrobot with multi-DOFs locomotion for medical applications”, Proceedings of 2012 IEEE International Conference on Mechatronics and Automation, pp.2405-2410, 2012.

[14] T Okada, S Guo, F Qiang, “A wireless microrobot with two motions for medical applications”, Proceedings of the 2013 ICME International Conference on Complex Medical Engineering, pp.306-311, 2012.

[15] J Guo, S Guo, X Wei, “Development of a New Kind of Magnetic Field Model for Wireless Microrobots”, Proceedings of the 2013 ICME International Conference on Complex Medical Engineering, pp.580-585, 2013.

[16] Y Zhang, K Zhang, L Zhang, “Spiral drive characteristics of a micro robot inside human body,” International Journal of Robot, Vol. 28, pp.560-570, 2006.